Hydrolysis of Zirconium and Hafnium Siloxide Complexes. Isolation and Characterization of the Intermediate Aqua Complexes $M[OSi(O^tBu)_3]_4(H_2O)_n$ (M = Zr, Hf; n = 1, 2)

Claus G. Lugmair and T. Don Tilley*

Department of Chemistry, University of California, Berkeley, California 94720-1460, and Chemical Sciences Division, Lawrence Berkeley Laboratory, 1 Cyclotron Road, Berkeley, California 94720

Received September 24, 1997

Hydrolysis of the tris(*tert*-butoxy)siloxy complexes $M[OSi(O^tBu)_3]_4$ (**1**, M = Zr; **2**, M = Hf) was studied. Careful addition of 1 or 2 equiv of water to THF solutions of **1** and **2** produced the isolable aqua complexes $M[OSi(O^tBu)_3]_4(H_2O)$ (**3**, M = Zr; **4**, M = Hf) and $M[OSi(O^tBu)_3]_4(H_2O)_2$ (**5**, M = Zr; **6**, M = Hf). These complexes are stable for weeks in solution and are stable indefinitely in the solid state. In solution, the aqua ligands in **3**−**6** are labile. Crystals of **4** are monoclinic ($C2/c$) with a = 62.2352(4) Å, b = 13.3362(2) Å, c = 27.0940(4) Å, β = 103.535(1)°, V = 21836.0(4) Å^3, and Z = 4. Addition of excess water to solutions of **5** and **6** at room temperature results in rapid hydrolysis to form a $MO_x(OH)_y(OH_2)_z$ gel and $HOSi(O^tBu)_3$. Below 10 °C in tetrahydrofuran-d_8, however, hydrolysis does not occur at an appreciable rate. At low temperatures, the rate of exchange between the aqua ligands of **5** and excess free water was found to depend on the water concentration. This indicates that the aqua ligand exchange occurs by an associative mechanism involving a seven-coordinate intermediate. On the basis of this observation, we postulate that the hydrolysis of **5** also proceeds via the tris(aqua) intermediate $Zr[OSi(O^tBu)_3]_4(H_2O)_3$. Compounds **3**−**6** are more thermally stable than **1** and **2**, indicating that the elimination of isobutene from the latter complexes is facilitated by a free coordination site on the Lewis acidic metal center.

Introduction

The sol−gel process represents a powerful method for preparing metal oxide films, fibers, and monoliths.[1] Such materials can have several unique properties, depending on their microstructure, composition, and crystallization behavior. A wider range of properties are accessible via well-mixed (homogeneous) multicomponent oxide materials, which may also be obtained by the sol−gel process. However, synthetic routes to these more complex systems must involve the controlled, homogeneous incorporation of the various components into the oxide network. This may be accomplished by matching hydrolysis rates for the alkoxide precursors via chemical modification of ligands.[1a,f] Alternatively, prehydrolysis of the less reactive precursor can be used to achieve a homogeneously mixed ceramic.[1a,f] Homogeneous, mixed-oxide gels have also been prepared by the hydrolysis of heterometallic alkoxide precursors of the type $M(OR)_nM'(OR)_m$.[2] These "single-source precursors" contain preformed M−O−M′ linkages which may facilitate formation of highly homogeneous ceramics. For example, this technique has been applied to the synthesis of aluminosilicate gels that transform to mullite at relatively low temperatures.[3]

The matching of hydrolysis rates for various M−OR linkages could in general be aided by knowledge of the kinetics and mechanisms for metal alkoxide hydrolysis reactions. The sol−gel chemistry of silicon alkoxides is well understood,[1,4] but little is known concerning the hydrolysis and condensation mechanisms for transition-metal or mixed-metal alkoxides.[5] The inherently rapid hydrolysis rates for transition metal alkoxides makes the study of the temporal evolution of these systems by spectroscopic methods very difficult. Kinetic data for these systems have therefore been limited to measurements of the onset time for gelation or the rate of precipitate particle growth.[6]

Bradley et al. have shown that the partial hydrolysis of transition metal alkoxide and trimethylsiloxide complexes results in the formation of soluble, oligomeric and polymeric oxo-

(1) (a) Brinker, C. J.; Scherer, G. W. *Sol-Gel Science*; Academic Press: Boston, MA, 1990. (b) *Sol-Gel Technology for Thin Films, Fibers, Preforms, Electronics, and Specialty Shapes;* Klein, L. C., Ed.; Noyes: Park Ridge, NJ, 1988. (c) Corriu, R. J. P.; Leclercq, D. *Angew. Chem., Int. Ed. Engl.* **1996**, *35*, 1421. (d) Guglielmi, M.; Carturan, G. *J. Non-Cryst. Solids* **1988**, *100*, 16. (e) Brinker, C. J. *J. Non-Cryst. Solids* **1988**, *100*, 31. (f) Schmidt, H. *J. Non-Cryst. Solids* **1988**, *100*, 51. (g) Sanchez, C.; Livage, J.; Henry, M.; Babonneau, F. *J. Non-Cryst. Solids* **1988**, *100*, 65.

(2) (a) Williams, A. G.; Interrante, L. V. In *Better Ceramics Through Chemistry;* Brinker, C. J., Clark, D. E., Ulrich, D. R., Eds.; Materials Research Society Symposia Proceedings, Vol. 32; North-Holland: New York, 1984; p 152. (b) Apblett, A. W.; Warren, A. C.; Barron, A. R. *Chem. Mater.* **1992**, *4*, 167. (c) Chaput, F.; Lecomte, A.; Dauger, A.; Boilot, J. P. *Chem. Mater.* **1989**, *1*, 199. (d) Mehrotra, R. C. *J. Non-Cryst. Solids* **1990**, *121*, 1. (e) Hubert-Pfalzgraf, L. G. *New. J. Chem.* **1987**, *11*, 663. (f) Bradley, D. C. *Polyhedron* **1994**, *13*, 1111. (g) Chandler, C. D.; Roger, C.; Hampden-Smith, M. J. *Chem. Rev.* **1993**, *93*, 1205.

(3) (a) Miller, J. B.; Tabone, E. R.; Ko, E. I. *Langmuir* **1996**, *12*, 2878. (b) Treadwell, D. R.; Dabbs, D. M.; Aksay, I. A. *Chem. Mater.* **1996**, *8*, 2056. (c) Pouxviel, J. C.; Boilot, J. P. In *Ultrastructure Processing of Advanced Ceramics*; Mackenzie, J. D., Ulrich, D. R., Eds.; Wiley: New York, 1988; p 197. (d) Pouxviel, J. C.; Boilot, J. P.; Dauger, A.; Huber, L. *Mater. Res. Soc. Symp. Proc.* **1986**, *73*, 269.

(4) Assink, R. A.; Kay, B. D. *J. Non-Cryst. Solids* **1988**, *99*, 359.

(5) (a) Livage, J.; Henry. M.; Sanches, C. *Prog. Solid State Chem.* **1988**, *18*, 259. (b) Livage, J.; Henry, M In *Ultrastructure Processing of Advanced Ceramics;* Mackenzie, J. D., Ulrich, D. R., Eds.; Wiley: New York, 1988.

(6) (a) Larbot, A.; Hours, T.; Bergez, P.; Charpin, J.; Cot, L. *J. Non-Cryst. Solids* **1992**, *147*−*148*, 85. (b) Hartel, R. W.; Berglund, K. A. In *Better Ceramics Through Chemistry, II*; Brinker, C. J., Clark, D. E., Ulrich, D. R., Eds.; Materials Research Society Symposia Proceedings, Vol. 73; Pittsburgh, PA, 1986; p 633. (c) Barringer, E. A.; Bowen, H. K. *Langmuir* **1985**, *1*, 414. (d) Davies, L.; Daza, L.; Grange, P. *J. Mater. Sci.* **1995**, *30*, 5087.

S0020-1669(97)01211-1 CCC: $15.00 © 1998 American Chemical Society
Published on Web 01/31/1998

(alkoxide)s and oxo(siloxide)s.[7] On the basis of solution molecular weight studies, they proposed structural models for these polymeric species. They also found that metal siloxides hydrolyze more slowly than metal alkoxides and form more condensed oligomers.[7,8] In some cases, the careful hydrolysis of metal alkoxides has led to the isolation and structural characterization of metal oxo(alkoxide) clusters.[9]

We have been exploring the use of $M[OSi(O^tBu)_3]_4$ (M = Zr (**1**), Hf (**2**)) complexes as single-source precursors to zirconia− and hafnia−silica materials.[10] In the solid state, these compounds undergo clean pyrolytic conversions under mild conditions (100−200 °C) to highly homogeneous $MO_2{\cdot}4SiO_2$ materials (e.g., eq 1). Thermolysis of these compounds in

$$\underset{\mathbf{1}}{Zr[OSi(O^tBu)_3]_4} \xrightarrow[10^{-3}\ \text{mm Hg}]{190\text{-}200\ ^\circ C} ZrO_2{\bullet}4SiO_2 + 12\ CH_2{=}CMe_2 + 6\ H_2O \quad (1)$$

anhydrous organic solvents produces high surface area gels that also appear to be highly homogeneous. In the solid state, the primary elimination products are isobutene and water, but in solution, some silanol, $HOSi(O^tBu)_3$, is also produced. To investigate the interaction of **1** and **2** with water and to evaluate the potential of these complexes as sol−gel precursors, we initiated the investigation described here.

Results

The addition of 30 equiv of H_2O to a THF-d_8 solution of **1** produced a clear gel within 20 min, and the quantitative formation of $HOSi(O^tBu)_3$ was observed by ^1H NMR spectroscopy. At this point, no other hydrolysis products (metal oxo(siloxide) complexes, HO^tBu, etc.) and no $M[OSi(O^tBu)_3]_4(H_2O)_x$ species were observed. These results indicate that the gel is a silica-free, hydrated zirconium oxide (eq 2).

$$\underset{\mathbf{1}}{Zr[OSi(O^tBu)_3]_4} \xrightarrow[\text{THF-}d_8]{\text{excess } H_2O} Zr_aO_b(OH)_c(OH_2)_d + 4\ HOSi(O^tBu)_3 \quad (2)$$

Careful addition of 1 or 2 equiv of water to **1** and **2** produced the isolable aqua complexes $M[OSi(O^tBu)_3]_4(H_2O)$ (**3**, M = Zr; **4**, M = Hf) and $M[OSi(O^tBu)_3]_4(H_2O)_2$ (**5**, M = Zr; **6**, M = Hf; eq 3),[11] which are extremely soluble in hydrocarbon solvents. These complexes were isolated in 52−76% yield after crystallizations from pentane. The aqua ligands give rise to distinct ^1H NMR resonances between 7.2 and 7.6 ppm and display ν(O−H) stretching vibrations in their infrared spectra at ca. 3230 cm^{-1}. The coordination geometry indicated in eq 3 for **5** and **6** is based on a preliminary crystal structure analysis of **6**. Despite considerable disorder in the structural model, it is clear that the water ligands adopt cis positions in an

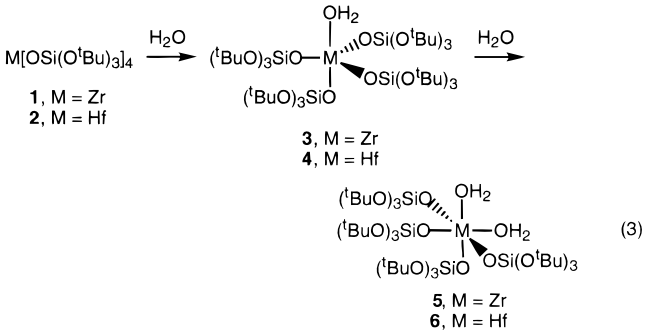

(3)

approximately octahedral coordination sphere. Analysis of the crude product from the synthesis of **5** by ^1H NMR spectroscopy revealed that only about 5% of the starting material had been hydrolyzed to give $HOSi(O^tBu)_3$. When 3 equiv of water was added to **1**, more of the silanol was formed at the expense of **5**, and no other products were detected by ^1H NMR spectroscopy.

Complexes **5** and **6** are stable in benzene-d_6 for weeks at room temperature. Even so, the aqua ligands in **3**−**6** are quite labile, as indicated by several observations. First, an equimolar mixture of **2** and **6** in benzene-d_6 rapidly and quantitatively forms **4** (by NMR spectroscopy). Furthermore, an equimolar mixture of **4** and **6** in toluene-d_8 at room temperature gave a spectrum with only one peak assigned to the aqua ligands (at δ 7.56). Cooling the sample led to decoalescence of this peak at 12.5 °C ($\Delta G^\ddagger$ = 14.3(1) kcal mol^{-1}), and the low-temperature spectrum at −20 °C contains resonances for the aqua ligands of **4** and **6** in a 1:2 intensity ratio (at δ 7.77 and 7.67, respectively). At this temperature, **4** displays a singlet for the siloxide ligand at δ 1.53, whereas **6** gives rise to two equal-area peaks for the siloxy ligands at δ 1.58 and 1.49. The presence of inequivalent siloxide ligands in **6** is consistent with the structure observed in the solid state.

To investigate the hydrolysis chemistry of **3**−**6**, the behavior of these compounds was examined in THF-d_8, which was expected to be a better solvent for both water and aqua complexes **3**−**6**. The dissolution of **3** in THF-d_8 resulted in rapid (<5 min), partial hydrolysis, as signaled by the formation of silanol (to produce a 2:1 molar ratio of **3** to silanol). A resonance at δ 1.35 (in a 1:4.5 integrated ratio with **3**) may be associated with a hydrolysis product. This product may also give rise to a resonance at δ 7.49, which is observed only after cooling the sample to −20 °C and is attributed to coordinated water. At −60 °C, the peak at δ 7.49 has a 1:8 integrated ratio with the peak for the aqua ligand of **3**. The ratio of **3** to silanol does not change over the course of at least 1 week at room temperature. The greater sensitivity of **3** (and **5**) toward hydrolysis in THF-d_8 may result from the nucleophilic and/or polar properties of THF, which could promote the elimination of silanol (vide infra). For comparison, the water-free complex **1** produces no silanol upon dissolution in THF-d_8.

When **5** was dissolved in THF-d_8, more silanol formed (to give a **5**:silanol molar ratio of 1.14), along with the species resonating at δ 1.35 (in a 1:2.6 integrated ratio with **5**). The resonance at δ 7.49, observed at −20 °C, appears slightly downfield from the resonance for the aqua ligand of **5** (Figure 1). At −60 °C, the peak at δ 7.49 has a 1:4 integrated ratio with the peak for the aqua ligand of **5**. In addition, a very small peak at δ 1.40 was observed. The putative hydrolysis product (δ 1.35) is more reactive than **5** toward hydrolysis, as indicated by its faster disappearance upon addition of more water. In ^1H NMR spectra of **3** and **5** at various temperatures (down to −60 °C), free water was not observed.

(7) (a) Bradley, D. C. *Coord. Chem. Rev.* **1967**, *2*, 299. (b) Bradley, D. C.; Carter, D. G. *Can. J. Chem.* **1961**, *39*, 1434. (c) Bradley, D. C.; Prevedorou-Demas, C. *J. Chem. Soc.* **1964**, 1580. (d) Bradley, D. C.; Carter, D. G. *Can. J. Chem.* **1962**, *40*, 15.
(8) English, W. D.; Sommer, L. H. *J. Am. Chem. Soc.* **1955**, *77*, 170.
(9) (a) Morosin, B. *Acta Crystallogr.* **1977**, *B33*, 303. (b) Day, V. W.; Eberspacher, T. A.; Klemperer, W. G.; Park, C. W.; Rosenberg, F. S. *J. Am. Chem. Soc.* **1991**, *113*, 8190.
(10) (a) Terry, K. W.; Tilley, T. D. *Chem. Mater.* **1991**, *3*, 1001. (b) Terry, K. W.; Lugmair, C. G.; Tilley, T. D. *J. Am. Chem. Soc.* **1997**, *119*, 9745.
(11) The proposed structures for **5** and **6** in eq 2 are based on a single-crystal X-ray diffraction analysis, which gave a highly disordered structure that appeared to contain approximately octahedral complexes with cis water ligands.

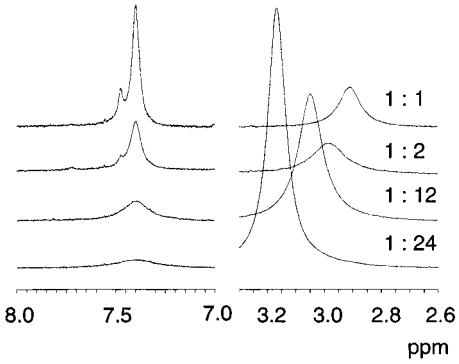

Figure 1. ^{1}H NMR spectra showing the resonances for the coordinated aqua ligands in complex **5** (7.4 ppm) and free water (ca. 3 ppm), at the indicated bound-to-free water ratios. All spectra were taken at −40 °C. The peak areas have not been normalized.

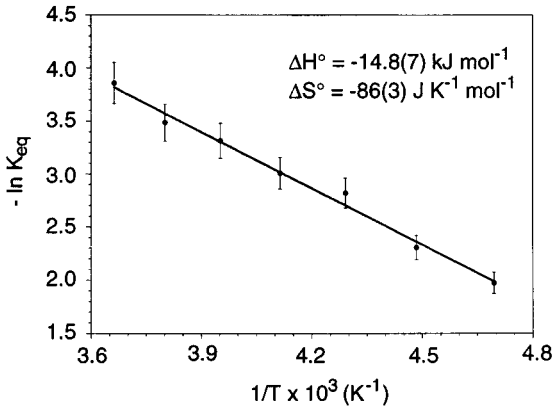

Figure 2. Van't Hoff plot for the disproportionation of **3** to **1** and **5**.

Cooling a THF-d_8 solution of **3** to 5 °C results in decoalescence of the resonance for the aqua ligand to separate peaks for **3** and **5**. As the temperature is lowered, the relative concentration of **5** increases. This indicates that, in THF-d_8, **3** is in equilibrium with the disproportionation products **1** and **5** (eq 4). To determine the equilibrium constant for the reaction

$$\underset{\mathbf{3}}{2\ Zr[OSi(O^tBu)_3]_4(H_2O)} \rightleftharpoons \underset{\mathbf{1}}{Zr[OSi(O^tBu)_3]_4} + \underset{\mathbf{5}}{Zr[OSi(O^tBu)_3]_4(H_2O)_2} \quad (4)$$

of eq 4, the integrated ratios of the ^{1}H NMR peaks for the aqua ligands were used to obtain the relative ratio of **3** to **5**. The concentration of **1** was assumed to be equal to the concentration of **5**. From a van't Hoff plot of the equilibrium data obtained between 0 and −60 °C, $\Delta H°$ and $\Delta S°$ were calculated to be −14.8(7) kJ mol^{-1} and −86(3) J K^{-1} mol^{-1}, respectively (Figure 2). In toluene-d_8, the disproportionation of **3** is also observed at low temperature. A van't Hoff plot of the equilibrium data obtained in this solvent gives $\Delta H° = -1.2(3)$ kJ mol^{-1} and $\Delta S° = -25(2)$ J K^{-1} mol^{-1}. The greater enthalpic driving force and loss of entropy in THF vs toluene suggest a greater degree of solvation for the disproportionated species on the right of eq 4. This may be at least partially due to the coordination of THF to **1**; however, such an adduct could not be isolated. Thus, dissolution of **1** in THF followed by removal of the solvent under vacuum gave a sample containing only THF-free complex **1** (by ^{1}H NMR spectroscopy). Therefore complex **1** does not form an isolable adduct with THF, probably because of the steric congestion provided by the siloxide ligands.

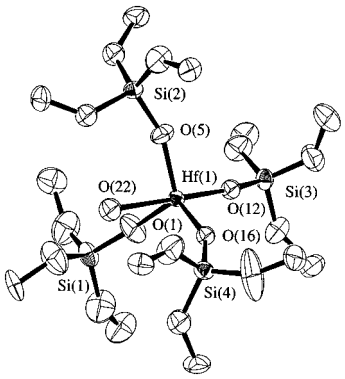

Figure 3. ORTEP view of **4**. Primary carbons and hydrogens have been removed for clarity. Disordered atoms with 20% probability have also been removed for clarity. Thermal ellipsoids are drawn at 50% probability.

Table 1. Selected Interatomic Distances (Å) and Angles (deg) for $Hf[OSi(O^tBu)_3]_4(H_2O)$ (**4**)

(a) Bond Distances			
Hf(1)−O(1)	1.908(6)	Hf(1)−O(5)	1.952(6)
Hf(1)−O(12)	1.937(7)	Hf(1)−O(16)	1.966(7)
Hf(1)−O(22)	2.322(8)	Hf(1)−O(23)	2.42(3)
Si(1)−O(1)	1.589(7)	Si(3)−O(12)	1.594(7)
Si(2)−O(5)	1.584(6)	Si(4)−O(16)	1.585(7)
(b) Bond Angles			
O(1)−Hf(1)−O(5)	116.9(3)	O(1)−Hf(1)−O(12)	102.8(3)
O(1)−Hf(1)−O(16)	120.2(3)	O(1)−Hf(1)−O(22)	75.6(3)
O(1)−Hf(1)−O(23)	61.2(8)	O(5)−Hf(1)−O(12)	102.7(3)
O(5)−Hf(1)−O(16)	111.0(3)	O(5)−Hf(1)−O(22)	77.5(3)
O(5)−Hf(1)−O(23)	171.5(8)	O(12)−Hf(1)−O(16)	99.2(3)
O(12)−Hf(1)−O(22)	178.3(3)	O(12)−Hf(1)−O(23)	70.5(8)
O(16)−Hf(1)−O(17)	24.0(8)	O(16)−Hf(1)−O(22)	82.3(3)
O(16)−Hf(1)−O(23)	75.8(8)	O(22)−Hf(1)−O(23)	109.2(8)
Hf(1)−O(1)−Si(1)	163.9(5)	Hf(1)−O(5)−Si(2)	159.7(4)
Hf(1)−O(12)−Si(3)	164.1(5)	Hf(1)−O(16)−Si(4)	153.0(5)

Variable-temperature ^{1}H NMR spectra of a sample of **5** in THF-d_8 do not contain resonances for **3**. At room temperature, the resonance for the aqua ligand is very broad, indicating an equilibrium involving **5**, **3**, and free water (eq 5). At −20 °C,

$$\underset{\mathbf{5}}{Zr[OSi(O^tBu)_3]_4(H_2O)_2} \rightleftharpoons \underset{\mathbf{3}}{Zr[OSi(O^tBu)_3]_4(H_2O)} + H_2O \quad (5)$$

the resonance for the aqua ligand sharpens considerably. Below −40 °C, there are two siloxide resonances for **5**, as there are in toluene-d_8. In toluene-d_8, the resonance for the aqua ligand of **5** is sharp at room temperature, indicating that the equilibrium of eq 5 lies far to the left in this solvent.

Single-Crystal X-ray Structure of 4. Complex **4** crystallizes from toluene (−40 °C) in the space group *C*2/*c*. The asymmetric unit contains 1.5 formula units of **4** and a molecule of toluene solvate. The independent complexes, one of which lies on a 2-fold axis, have similar coordination geometries which may be described as distorted trigonal bipyramids. Both molecules possess considerable disorder, which was modeled successfully as resulting from the superposition of two orientations of the structure at each site. An ORTEP drawing of a complete molecule, representing the major contributor to the complex containing Hf(1), is given in Figure 3. Important bond distances and angles are collected in Table 1. The degree of disorder introduces considerable error into the metrical parameters, but it is clear that the trigonal bipyramids are distorted such that equatorial siloxide ligands bend toward the axial H_2O ligand. For the structure in Figure 3, the O(22)−Hf(1)−O(12)

angle is 178° and the angles in the equatorial plane range from 111 to 120°. The average O(H_2O)−Hf(1)−O(eq) and O(eq)−Hf(1)−O(12) angles in this structure are 78 and 102°, respectively. In other conformations of this molecule in the structure, the geometrical parameters are similar. The Hf−O(siloxide) bond distances range from 1.908(6) to 1.966(7) Å and are comparable to the corresponding distances in Hf[OSi(O^{t}Bu)$_3$]$_4$.[10b] As expected, the Hf−OH_2 bond distances are significantly longer (Hf(1)−O(22) = 2.322(8) Å; Hf(1)−O(23) = 2.42(3) Å).

Interaction of 5 with Excess Water. The high stability of **3**−**6** suggests that the hydrolysis of **1** and **2** occurs via initial formation of the bis(aqua) adducts. To investigate subsequent steps in the hydrolysis, an attempt was made to monitor the reaction of **5** with water by ^{1}H NMR spectroscopy. As stated previously, the addition of excess water to a THF-d_8 solution of **1** resulted in complete hydrolysis of **1** with formation of HOSi(O^{t}Bu)$_3$ within 20 min at room temperature. However, resonances for **5** and the hydrolysis product HOSi(O^{t}Bu)$_3$ are not well resolved, which prevents the accurate integration of these peaks during the course of reaction.

In THF-d_8 solution, complex **5** does not hydrolyze below 10 °C in the presence of excess water. This allowed an investigation of the exchange between free water and the aqua ligands of complex **5** by variable-temperature ^{1}H NMR spectroscopy. Due to the hydrolysis of **5** above 10 °C, it was not possible to observe the complete range of coalescence behavior. At 10 °C, **5** in the presence of 2 equiv of water gives rise to a spectrum in which the resonances for free and bound water were too broad to be observed. As this sample was cooled, the peak for bound water (7.33 ppm) was observed to first emerge at about −10 °C, and the peak for free water (2.81 ppm) was first observed at −20 °C. As the sample was cooled further, both resonances sharpened considerably. Even though coalescence temperatures could not be well defined, we attribute this behavior to exchange between free and bound water.

To determine the influence of the free water concentration on the rate of ligand exchange, the NMR line shapes were monitored as a function of water concentration in THF-d_8. Figure 1 shows regions of the ^{1}H NMR spectra containing bound and free H_2O resonances for samples of **5** with various concentrations of free water at −40 °C. The resonance for coordinated water broadens drastically as the free water concentration increases. This effect of water concentration on the rate of exchange indicates that the rate-limiting step involves free water. This is consistent with an associative mechanism in which the rate-limiting step is a bimolecular reaction to form a seven-coordinate intermediate. If the ligand exchange were occurring by a dissociative mechanism through a five-coordinate intermediate (complexes **3** and **4**), then the rate-limiting step would involve ligand dissociation. In this case, the rate of ligand exchange would be independent of the free water concentration.

An attempt was made to follow the hydrolysis of **5** in toluene-d_8, despite the marginal solubility of water in this solvent. Addition of 30 equiv of water to a toluene-d_8 solution of **5** resulted in rapid hydrolysis of **5**, with formation of HOSi(O^{t}Bu)$_3$ (by ^{1}H NMR spectroscopy) and a heterogeneous mixture. Minor amounts of other OSi(O^{t}Bu)$_3$-containing products were indicated by the appearance of new ^{1}H NMR resonances near 1.5 ppm. Within 5 min, a gel-containing aqueous phase, presumed to contain $ZrO_x(OH)_y(OH_2)_z$, had appeared. This gel seems to act as a desiccant, since upon its formation the hydrolysis slows dramatically and is halted prematurely. Thus, after 15 min, 33% of **5** was consumed, but after 60 min, only 40% of **5** had converted. A larger excess of water did not significantly change the extent of hydrolysis. Interestingly, the amount of HOSi(O^{t}Bu)$_3$ produced during this reaction is low compared to the theoretically expected values based on complete conversion of **5**, suggesting that siloxy(hydroxy)zirconium clusters may condense from solution.

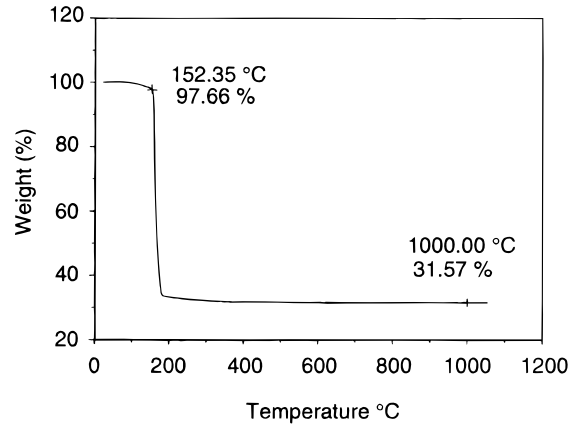

Figure 4. TGA trace for **3** under N_2, with a heating rate of 10 °C min^{-1}.

Solid-State Thermolyses of 3 and 5. The TGA curve for **3** reveals a small (2.3%) weight loss from 90 to 152 °C, followed by a more dramatic weight loss with an onset temperature of 152.4 °C (Figure 4). The ceramic yield at 1000 °C is 31.57%, which corresponds to quantitative formation of $ZrO_2{\cdot}4SiO_2$ (31.26%). The volatile products trapped from thermolysis of **3** for 5 min at 130 °C under vacuum consisted of 0.26 equiv of H_2O, 0.06 equiv of isobutene, 0.06 equiv of *tert*-butyl alcohol, and 0.04 equiv of HOSi(O^{t}Bu)$_3$ (by ^{1}H NMR spectroscopy). These results indicate that the initial weight loss below 152 °C involves dehydration, accompanied by a slight amount of silanol elimination. The TGA curve for the bis(aqua) complex **5** is nearly identical in appearance to that for **3**, except that the initial weight loss between 50 and 152 °C is slightly greater (ca. 3.1%) and closely corresponds to the 3.05% weight loss expected for total dehydration. However, a bulk sample of **5** heated to 135 °C for 5 min under vacuum released only 0.78 equiv of H_2O, along with 0.07 equiv of isobutene, 0.02 equiv of *tert*-butyl alcohol, and 0.01 equiv of the silanol. The remaining nonvolatile material was primarily **3** (by NMR spectroscopy). Compound **5** undergoes a precipitous weight loss at 152.1 °C, and the ceramic yield at 1000 °C (30.99%) is close to the theoretical yield for $ZrO_2{\cdot}4SiO_2$ (30.78%).

The water adducts **3** and **5** therefore undergo decomposition at a higher temperature than does the parent complex Zr[OSi(O^{t}Bu)$_3$]$_4$, which has an onset temperature for decomposition at 137 °C.[10] Thus, it seems that the coordinated water ligands in **3** and **5** stabilize the complexes to some degree, probably by creating a less coordinatively unsaturated environment. Also, the trapping experiments suggest that initial intramolecular hydrolysis is competitive with pyrolytic decomposition of the siloxide ligands.

Discussion

The aqua complexes **3**−**6** form with relatively little hydrolysis of the precursors **1** and **2**, and the moderate isolated yields for these compounds stem from their high solubility in organic solvents. In these complexes, the aqua ligands are quite labile, as demonstrated by variable-temperature NMR studies which reveal the rapid exchange of H_2O ligands between **4** and **6**. We were therefore somewhat surprised to find that these complexes

Scheme 1

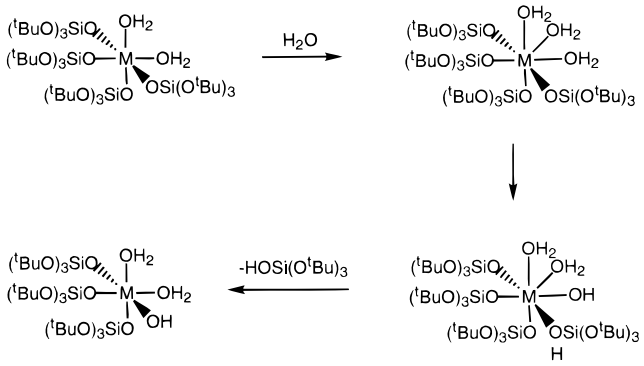

are stable indefinitely in the solid state and are stable for weeks in solution. A small number of other monomeric aqua complexes of zirconium and hafnium have been isolated, such as $(\eta^5\text{-}C_5H_5)_2Zr(H_2O)_3(CF_3SO_3)_2(THF)$.[12] Of course, the aqueous coordination chemistry of zirconium and hafnium has produced a number of aqua complexes.[13]

In contrast to $(^sBuO)_2AlOSi(OEt)_3$, which has been shown to be a good precursor for the preparation of homogeneous aluminosilicate gels,[3] the zirconium and hafnium siloxide complexes reported here do not give mixed-element oxide gels upon hydrolysis. Whereas the aluminum complex may undergo sol−gel polymerization via hydrolysis of the Al−O^{s}Bu linkages, the zirconium and hafnium compounds neccessarily cleave their M−O−Si heterolinkages upon hydrolysis. The hydrolytic stability of the $-OSi(O^tBu)_3$ group results in the loss of silanol as a stable byproduct, such that silicon is not incorporated into the gel structure. The unreactive nature of the silicon centers in **1** and **2** makes these complexes behave more like metal alkoxides in their hydrolysis chemistry.

It is generally assumed that transition metal alkoxides hydrolyze by a "nucleophilic substitution" mechanism in which a water molecule first coordinates to the metal center. This step is followed by an intramolecular proton transfer from the coordinated water molecule to an alkoxide ligand and then elimination of the resulting alcohol ligand.[5] However, such processes have not been directly observed, and very little mechanistic information is available. In the hydrolysis of **1** and **2**, the mono- and bis(aqua) adducts **3**−**6** appear to be stable intermediates. Given the stability of **3**−**6** toward silanol elimination in solution and the rapid hydrolysis of **5** and **6** by free water, it appears that the aqua ligands in **5** and **6** are not directly involved in the rate-determining step for hydrolysis of these complexes. Furthermore, these results suggest that silanol is formed in a bimolecular reaction between **5** (or **6**) and H_2O. Given the precedent of seven- and eight-coordinate zirconium complexes,[13] it appears that these hydrolyses could occur via a seven-coordinate intermediate (Scheme 1). Variable-temperature ^1H NMR studies of **5** indicate that exchange between coordinated and free water proceeds by an associative mechanism. This lends further support to the hypothesis that the mechanism for hydrolysis of **5** also proceeds through an associative mechanism and a seven-coordinate intermediate.

Finally, it is interesting to note that the coordination of water to **1** and **2** results in an increase in the thermal stability of these complexes. This suggests that the pyrolytic elimination of isobutene from **1** and **2** is initiated by a free coordination site on the Lewis acidic metal center. Compounds **5** and **6** are thermally sensitive, in that they readily lose 1 equiv of water upon brief heating to 135 °C. In contrast, **3** and **4** lose only 25% of the coordinated water under similar conditions.

Conclusion

The suitability of **1** and **2** as sol−gel precursors was examined by studying reactions of these complexes with water. These reactions rapidly produce zirconia or hafnia gels along with $HOSi(O^tBu)_3$, which is quite stable toward hydrolysis. Thus, compounds **1** and **2** are not good sol−gel precursors to homogeneous networks with significant quantities of M−O−Si linkages. Their hydrolysis chemistry is therefore more comparable to that of metal alkoxides $M(OR)_4$ (M = Zr, Hf) and related derivatives, which are important sol−gel precursors to zirconia and hafnia.[14] For the first time, we have been able to obtain information on the mechanism of hydrolysis for group 4 transition-metal complexes of the type $M(OR)_4$. This information strongly suggests an associative process in the rate-limiting step for hydrolysis.

Experimental Section

All manipulations were performed under an atmosphere of nitrogen using standard Schlenk techniques and/or in a Vacuum Atmospheres drybox. NMR spectra were recorded on a Bruker AMX400 (at 400 (^1H) or 100 (^{13}C) MHz) or a Bruker AMX 300 (at 300 (^1H) MHz). Infrared spectra were recorded on a Perkin-Elmer 1330 spectrophotometer. Thermolyses were performed using a Lindberg 1700 °C or a Lindberg 1200 °C three-zone tube furnace. Thermal analyses were performed on a Du Pont model 2000 thermal analysis system. Dry oxygen-free solvents were used throughout. Elemental analyses were performed at the College of Chemistry Microanalytical Facility. The compounds $M[OSi(O^tBu)_3]_4$ (M = Zr (**1**), Hf (**2**)) were prepared by the literature procedure.[10]

$Zr[OSi(O^tBu)_3]_4(H_2O)$ (3). A THF solution (15 mL) of H_2O (6.78 μL, 0.376 mmol) was added dropwise to a THF solution (20 mL) of **1** (0.431 g, 0.376 mmol). The reaction mixture was then stirred for 12 h. The solvent was removed in vacuo, and the resulting solid was kept under dynamic vacuum for 5 h. The product was extracted into pentane (20 mL), and concentration and cooling (−40 °C) of the pentane solution afforded 0.23 g of **3** as colorless crystals in 53% yield. Anal. Calcd for $C_{48}H_{110}O_{17}Si_4Zr$: C, 49.57; H, 9.53. Found: C, 49.17; H, 9.70. IR (CsI, Nujol, cm^{-1}): 3233 vbr, 1388 m, 1364 m, 1241 m, 1193 m, 1060 s, 1028 w sh, 1006 m sh, 948 s, 828 m, 805 w sh, 700 m, 649 w, 546 vw, 515 w sh, 496 w, 478, 466 w sh. ^1H NMR (400 MHz, benzene-d_6, 22 °C): δ 7.42 (2 H, H_2O), 1.52 (108 H, $OCMe_3$). $^{13}C\{^1H\}$ NMR (100 MHz, benzene-d_6, 22 °C): 72.67 (CMe_3), 32.10 (CMe_3).

$Hf[OSi(O^tBu)_3]_4(H_2O)$ (4). This compound was synthesized by the same procedure used for **3**, using a THF solution (20 mL) of H_2O (5.29 μL, 0.294 mmol) and a THF solution (20 mL) of **2** (0.362 g, 0.294 mmol). White colorless crystals of **4** were obtained in 54% yield (0.19 g). Anal. Calcd for $C_{48}H_{110}HfO_{17}Si_4$: C, 46.11; H, 8.87. Found: C, 45.85; H, 8.95. IR (CsI, Nujol, cm^{-1}): 3196 vbr, 1388 m, 1364 m, 1240 m, 1193 m, 1057 s, 1028 w sh, 1005 m sh, 972 s, 914 vw sh, 829 m, 700 m, 647 w, 547 vw, 515 w, 494 w, 478 w sh, 462 vw sh, 434 w. ^1H NMR (400 MHz, benzene-d_6, 22 °C): δ 7.63 (2 H, H_2O), 1.52 (108 H, $OCMe_3$). $^{13}C\{^1H\}$ NMR (100 MHz, benzene-d_6, 22 °C): 72.66 (CMe_3), 32.12 (CMe_3).

$Zr[OSi(O^tBu)_3]_4(H_2O)_2$ (5). The procedure for **3** was used, starting with a THF solution (20 mL) of H_2O (40.2 μL, 2.23 mmol) and a THF

(12) Thewalt, U.; Lasser, W. *J. Organomet. Chem.* **1984**, *276*, 341.
(13) Fay, R. C. In *Comprehensive Coordination Chemistry*; Wilkinson, G., Gillard, R. D., McCleverty, J. A., Eds.; Pergamon: Oxford, U.K., 1987; pp 384−387.
(14) (a) Ward, D. A.; Ko, E. I. *Chem. Mater.* **1993**, *5*, 956. (b) Miller, J. B.; Rankin, S. E.; Ko, E. I. *J. Catal.* **1994**, *148*, 673. (c) Okubo, T.; Nagamoto, H. *J. Mater. Sci.* **1995**, *30*, 749. (d) Ray, J.; Chatterjee, M.; Ganguli, D. *J. Mater. Sci. Lett.* **1992**, *11*, 968. (e) Toba, M.; Mizukami, F.; Niwa, S.; Sano, T.; Maeda, K.; Annila, A.; Komppa, V. *J. Mol. Catal.* **1994**, *94*, 85.

solution (20 mL) of **1** (1.28 g, 1.12 mmol). White colorless crystals were obtained in 76% yield (1.01 g). Anal. Calcd for $C_{48}H_{112}O_{18}Si_4Zr$: C, 48.82; H, 9.56. Found: C, 48.89; H, 9.25. IR (CsI, Nujol, cm^{-1}): 3381 br sh, 3246 vbr, 1387 m, 1363 m, 1240 m, 1190 m, 1056 s, 1027 w sh, 1003 m sh, 956 s, 914 vw sh, 828 m, 698 m, 645 w, 545 vw, 516 w sh, 492 w, 479 w, 465 w sh, 424 w. ^{1}H NMR (400 MHz, benzene-d_6, 22 °C): δ 7.35 (4 H, H_2O), 1.53 (108 H, $OCMe_3$). $^{13}C\{^1H\}$ NMR (100 MHz, benzene-d_6, 22 °C): 72.78 (*C*Me$_3$), 32.04 (C*Me*$_3$).

Hf[OSi(O^{t}Bu)$_3$]$_4$(H$_2$O)$_2$ (6). The procedure for **3** was used, starting with a THF solution (20 mL) of H_2O (19.5 μL, 1.08 mmol) and a THF solution (20 mL) of **2** (0.666 g, 0.541 mmol). White colorless crystals of **6** were obtained in 52% yield (0.36 g). Anal. Calcd for $C_{48}H_{112}HfO_{18}Si_4$: C, 45.46; H, 8.90. Found: C, 45.37; H, 8.98. IR (CsI, Nujol, cm^{-1}): 3327 br sh, 3201 vbr, 1386 m, 1362 m, 1240 m, 1191 m, 1056 s, 1026 w sh, 1000 m sh, 973 s, 911 vw sh, 827 m, 698 m, 643 w, 545 vw, 517 w, 492 w, 479 w sh, 459 vw sh, 431 vw. ^{1}H NMR (400 MHz, benzene-d_6, 22 °C): δ 7.53 (4 H, H_2O), 1.53 (108 H, $OCMe_3$). $^{13}C\{^1H\}$ NMR (100 MHz, benzene-d_6, 22 °C): 72.67 (*C*Me$_3$), 32.05 (C*Me*$_3$).

Crystallographic Structure Determination. Crystallographic data are collected in Table 2. Crystals of **4** were grown from a concentrated toluene solution at −40 °C. At room temperature, the crystals fracture within 15 min. A colorless blocky crystal of dimensions 0.35 × 0.24 × 0.19 mm was mounted on a glass fiber using Paratone N hydrocarbon oil. The mounted crystal was placed under a cold stream of nitrogen on the diffractometer within 5 min of removing the crystals from a cold bath. A preliminary orientation matrix and unit cell parameters were determined by collecting sixty 10-s frames, followed by spot integration and least-squares refinement. A hemisphere of data was collected using a triclinic unit cell with ω scans of 0.3° and a collection time of 30 s per frame. Frame data were integrated (XY spot spread = 1.60°; Z spot spread = 0.60°) using SAINT. The data were corrected for Lorentz and polarization effects. An absorption correction was performed using XPREP ($\mu R = 0.20$, $T_{max} = 0.68$, $T_{min} = 0.59$). The data were found to conform to a *C*-centered monoclinic unit cell twice the volume of the triclinic cell. The 45 444 integrated reflections were averaged in point group 2/*m* to give 16 294 unique reflections ($R_{int} = 0.035$). Of these, 10 349 reflections were considered observed ($I > 4.00\sigma(I)$). No decay correction was necessary. The structure was successfully refined in the space group *C*2/*c*. The space group *Cc* was also tried without success. The structure was solved using direct methods (SIR92) and refined by full-matrix least-squares methods using teXsan software.

The asymmetric unit was found to contain 1.5 formula units of **4** along with one molecule of toluene. The one complete molecule within the asymmetric unit, containing Hf(1), was modeled with some of the oxygen atoms [O(7)−O(8); O(10)−O(9); O(12)−O(11); O(16)−O(17); O(20)−O(21)] disordered over two sites. Each pair of sites were modeled with 80% and 20% populations, respectively. The oxygen atom of the water molecule is also disordered over two sites, O(22) and O(23), with 80% and 20% populations, respectively. The primary carbon atoms of two −O^{t}Bu groups were also disordered over two sites.

The molecule containing Hf(2) is located on a 2-fold axis. In this molecule, all the carbon atoms in the −O^{t}Bu moieties were modeled in two positions each with 50% population. One of the primary carbon atoms was additionally disordered over two sites each with 25% population. The oxygen atom of the water molecule, O(32), was assigned 50% population. The atoms with full occupancies were refined anisotropically.

Table 2. Crystallographic Data for Hf[OSi(O^{t}Bu)$_3$]$_4$(H$_2$O) (**4**)

(a) Crystal Parameters	
compound	3(**4**)·2C_7H_8
empirical formula	$C_{158}H_{346}Hf_3O_{51}Si_{12}$
fw	3934.95
cryst color, habit	colorless, blocky
cryst size, mm	0.35 × 0.24 × 0.19
crystal system	monoclinic
space group	*C*2/*c*
a, Å	62.2352(4)
b, Å	13.3362(2)
c, Å	27.0940(4)
β, deg	103.535(1)
V, Å^3	21 863.0(4)
Z	4
ρ(calc), g cm^{-3}	1.195
μ(Mo Kα), cm^{-1}	15.49
temp, °C	−103
(b) Data Collection	
diffractometer	Siemens SMART
radiation (λ, Å)	Mo Kα (0.710 69)
scan type	ω (0.3° per frame)
scan rate	30.0 s per frame
no. of rflns collected	45 444
no. of unique rflns	16 294 ($R_{int} = 0.035$)
no. of observns	10 349 ($I > 4.00\sigma(I)$)
(c) Refinement	
rfln/param ratio	10.56
R^a	4.6
$R_w{}^b$	5.9
GOF	2.32
max/min peak in final diff map, e Å^{-3}	0.82/−0.71

$^a R = \sum||F_o| - |F_c||/|F_o|$. $^b R_w = [\sum w(|F_o| - ||F_c|)^2/\sum w(F_o)^2]^{1/2}$.

The number of variable parameters was 980, giving a data:parameter ratio of 10.56. The maximum and minimum peaks on the final difference Fourier map corresponded to 0.82 and −0.71 e Å^{-3}: $R = 0.046$, $R_w = 0.059$, GOF = 2.32.

Acknowledgment. This work was supported by the Director, Office of Energy Research, Office of Basic Energy Sciences, Chemical Sciences Division, of the U. S. Department of Energy under Contract No. DE-AC03-76SF00098.

Supporting Information Available: Tables of atomic coordinates, bond distances and angles, and anisotropic displacement parameters (16 pages). Ordering information is given on any current masthead page.

IC971211G